Low Temperature Physics/Fizika Nizkikh Temperatur, 2015, v. 41, No. 10, pp. 1054–1062

Thermoelectric spin transport through ferromagnetic heterostructures

Scott A. Bender

Department of Physics and Astronomy, University of California, Los Angeles, California 90095, USA
E-mail: sbender@ucla.edu

Received July 14, 2015, published online August 25, 2015

We study how spin is transferred by ferromagnetic dynamics in a charge insulator in response to a thermoelectric bias, which is established by supplying heat and/or spin accumulation via normal leads. At zero temperature, magnetic anisotropies pin the macroscopic order, which necessitates a finite threshold bias to induce a spin current in a steady state of unpinned dynamics. At finite temperatures, however, thermal spin waves provide a spin transport channel in response to a linear thermoelectric bias. The theoretical description is rooted in the Landau–Lifshitz–Gilbert phenomenology both for the macroscopic dynamics of the magnetic order and quantum kinetics of thermal magnons. In this paper we connect the classical and quantum aspects of the underlying magnetic dynamics and spin transport, as well as provide a unified view of the exchange mediated bias of spin Seebeck physics of the magnetic interface and bulk.

PACS: 75.30.Ds Spin waves;
75.70.Cn Magnetic properties of interfaces;
75.76.+j Spin transport effects.

Keywords: magnetic dynamics, spin transport, ferromagnetic heterostructures.

1. Introduction

Central to the field of spintronics is the transport of angular momentum across mesoscopic structures. In conducting devices, this is accomplished by spin polarized itinerant electrons, which carry spin angular momentum over finite distances by their translational motion. Traditionally, such spin polarized electronic currents are generated by electrical biasing, either by utilizing the fact that in the presence of ferromagnetic order, electrons, and therefore electric currents, are spin polarized [1–3], or more recently by exploiting the spin-orbit interaction to convert electric into spin currents [4–6]. Additionally, thermoelectric effects have opened the possibility of generating a spin polarized electronic current from a heat flux [7–12].

In electrically insulating materials, itinerant electron transport is gapped out. It is, however, still possible to transmit angular momentum in insulating ferromagnets via chargeless excitations of the magnetization (spin waves) [13–15]. If the ferromagnet is interfaced with a nonmagnetic (normal) metal, the localized magnetic moments of the former are coupled to the itinerant electrons of the latter along the interface, fostering the interconversion of ferromagnetic dynamics with spin polarized electric currents [16–19]. Hence, insulating ferromagnets may be used to carry pure spin signals (mediated by spin waves) between electronic device elements [20,21], potentially offering very different transport properties from their conducting counterparts. It is therefore essential to have a solid theoretical underpinning for transport within normal metal–ferromagnet heterostructures. This has previously been accomplished from a both a classical [22,23] and quantum [24,25].

In this review, we describe spin transport through a normal metal|ferromagnet|normal metal heterostructure driven by thermal or electrical biasing, connecting both the classical and quantum approaches. First, we briefly discuss how a structural thermal or spin accumulation bias is established in the normal metal leads. Next, we treat spin transport in the ferromagnet at zero temperature, as described by the Landau–Lifshitz–Gilbert (LLG) equation [26]; here, below a critical bias, magnetic dynamics are relaxed by a combination of Gilbert damping and spin pumping, and spin transport can only be facilitated in the steady-state of unpinned dynamics corresponding to an instability. Last, we extend the LLG phenomenology to thermal fluctuations of the spin density. In contrast to the zero temperature magnetic dynamics, at finite temperature, steady-state spin and heat currents, carried by thermally

activated magnons, may be driven in linear response to the biases established in the leads. We develop a quantum kinetic theory for bulk magnon transport, which, when complemented with the appropriate boundary conditions describing spin and heat transfer between the ferromagnet and leads, allows for a simple characterization of the linear response of the heterostructure.

2. Heterostructure biasing

Consider an insulating ferromagnet F of thickness d, which is bounded by normal metal contacts N_1 on the left and N_2 on the right (see Fig. 1). The structure is invariant under spatial translations in the yz plane, while the planes $x = 0$ and $x = d$ define the interfaces connecting F with leads N_1 and N_2, respectively. Spin transport across the $N_1|F|N_2$ structure can be driven two different ways. First, a nonequilibrium imbalance of itinerant electron spins, called a spin accumulation, may be created electrically in each metal by, e.g., nonlocal spin injection or spin Hall physics. Via the interfacial exchange interaction, this spin accumulation exerts a spin-transfer torque on the magnetization just inside F which is transferred by magnetic dynamics across F towards the other interface. Second, if a temperature gradient across the structure is established by heating or cooling the normal metal contacts, thermal fluctuations can drive angular momentum across each N_l–F interface (with $l = 1, 2$ for left and right), which is similarly carried across F.

A complete account of transport through the heterostructure, driven electrically and/or thermally, consists of three components: spin and heat transport (1) inside each metallic lead, (2) across each $N_l|F$ interface, and (3) through F. The first is a bulk theory, detailing how electrical and/or thermal biasing of a given metallic lead establishes (through coupled spin, charge and heat currents inside the lead) a spin accumulation and nonequilibrium phonon and electron temperatures along the interface with F. Spin and heat are then transferred, as characterized by the second theory (which takes the form of boundary conditions for spin and heat currents) from the N_l nonequilibrium electrons and phonons along the interface to F, where they are carried by the F magnetization $\mathbf{M}(\mathbf{r}, t)$ and phonons, as characterized by the third theory, describing bulk transport in F. The F magnetization, N spin accumulations, and electronic and phononic temperatures everywhere must all be obtained together self-consistently using both the bulk transport theories in N_1, N_2 and F along with the boundary conditions that link them.

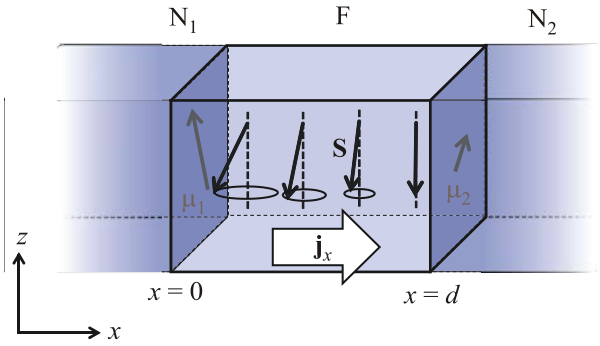

Fig. 1. (Color online) $N_l|F|N_2$ heterostructure at zero temperature, with electrically generated spin accumulations μ'_1 and μ'_2 along the interfaces inside the leads. At zero temperature, the spin density $\mathbf{s} = s\mathbf{n}$ has fixed magnitude, but may still carry a spin current. When one or both of the spin accumulations is sufficiently large, s is excited away from equilibrium ($\mathbf{n} = -\mathbf{z}$), and a steady state spin current $\mathbf{j}_x$, Eq. (5), (with a dc component $j_x^{(z)}$, Eq. (9)) flows in the x direction.

Such a program, however, can be simplified by employing a small number of assumptions. First, let us assume that electrons and phonons are strongly interacting within the normal metal leads, so that the phonon and electron temperatures there are the same. Second, as an electrical insulator, F may be expected to form the bottleneck for heat transport across the structure, relative to the highly thermally conductive metallic leads. A uniform temperature T_1 (T_2) is therefore established within the lead N_1 (N_2), which we take to be an experimentally tunable variable. Last, in the interest of simplicity, let us suppose that each lead is a perfect poor spin sink, in which case we may assume that any spin accumulation generated by magnetic dynamics is relaxed into the lattice of the normal metal by strong spin orbit interactions; hence, the spin accumulation along the interface, in this case, is generated electrically in the normal lead and may therefore be treated as an experimentally tunable variable. Under these assumptions, then, we therefore circumvent a detailed transport theory in leads and focus on transport in F and through the interfaces, which on the normal metal sides is determined by the experimentally fixed temperatures and spin accumulations in each [27].

3. Zero temperature dynamics

In this section we consider the case when the entire structure is at zero temperature. Here, the heterostructure may only be biased by the generation of a spin accumulation in one or both of the leads. We illustrate how a steady state spin current vanishes in linear response to the spin accumulations but may be established beyond a threshold bias.

At zero temperature, the state of the local magnetization $\mathbf{M} = M\mathbf{m}$ in F is specified entirely by the unit vector $\mathbf{m}$ and the saturation magnetization M. In the bulk, the dynamics of $\mathbf{m}$ are governed by the Landau–Lifshitz Gilbert equation:

$$\dot{\mathbf{m}} = -\gamma \mathbf{m} \times \mathbf{H}_{\text{eff}} + \alpha \mathbf{m} \times \dot{\mathbf{m}}, \qquad (1)$$

where γ is the gyromagnetic ratio and α is the unitless Gilbert damping parameter, describing the flow of spin out

of the magnetization and into other degrees of freedom of F (e.g. the lattice). The effective field is given by

$$\mathbf{H}_{\rm eff} = -\delta_{\mathbf{M}}\mathcal{F}, \tag{2}$$

where $\mathcal{F}$ is the free energy, which has four contributions:

$$\mathcal{F} = \frac{M}{\gamma\hbar}\int d^3r(A\mathbf{m}\cdot\nabla^2\mathbf{m} + Km_z^2 - Hm_z) + \mathcal{F}_d. \tag{3}$$

The first term in parenthesis is the exchange energy, parametrized by the exchange stiffness A, in units of energy times length squared. The second is the uniaxial crystalline anisotropy contribution to the energy, which is easy axis (easy plane) when $K > 0$ ($K < 0$). The third is the Zeeman energy due to an applied magnetic field $H\mathbf{z}$, which for simplicity is applied along the easy axis, $\mathbf{z}$, of the magnet. The last term, $\mathcal{F}_d$ is the dipolar energy. For long wavelength excitations of the magnetization, which are generally the relevant modes excited by spin-transfer torque at zero temperature, the dipolar energy may be expressed in terms of the demagnetization tensor, which can be absorbed into K provided that the magnet is approximately rotationally invariant around the z-axis; we shall therefore disregard the dipole energy $\mathcal{F}_d$.

Because we are concerned with the transfer of angular momentum, it is convenient to change to the spin density $\mathbf{s} = -\mathbf{M}/\gamma = s\hbar\mathbf{n}$, where $\mathbf{n}$ is a unit vector, and $s = M/\gamma\hbar$ is the saturation spin density in units of $\hbar$. Upon multiplying by $s\hbar$, Eq. (1) becomes:

$$s(1+\alpha\mathbf{n}\times)\hbar\dot{\mathbf{n}} + s(H + Kn_z)\mathbf{n}\times\mathbf{z} + \partial_i\mathbf{j}_i = 0, \tag{4}$$

where summation over the spatial index $i = x, y, z$ is implied, and

$$\mathbf{j}_i = -sA\mathbf{n}\times\partial_i\mathbf{n} \tag{5}$$

is the spin current flowing in the direction i. The z component Eq. (4) has the form of a local conservation equation for spin, with a sink term $\propto\alpha$. The components of Eq. (4) orthogonal to $\mathbf{z}$ are not conserved because the magnetic field and anisotropy break the rotational invariance of the magnet.

We take the magnetic field to be sufficiently strong ($H > K$) that in equilibrium, $\mathbf{n} = -\mathbf{z}$. At zero temperature, only by spin-transfer torque can magnetic dynamics be excited away from equilibrium and angular momentum transferred through F to and from the metal leads. The spin-transfer torque at the interface of F with N_l, which arises from the spin accumulation there, is parametrized by the complex spin mixing conductance $g_l^{\uparrow\downarrow} = g_{r,l}^{\uparrow\downarrow} + ig_{i,l}^{\uparrow\downarrow}$ (with units of inverse area) for that interface and appears in the form of a boundary condition on spin current $\mathbf{j}_i$ [28]. The spin current passing into and out of F from the leads is [19]:

$$\frac{1}{4\pi}(g_{i,1}^{\uparrow\downarrow} + g_{r,1}^{\uparrow\downarrow}\mathbf{n}\times)(\boldsymbol{\mu}_1'\times\mathbf{n} - \hbar\dot{\mathbf{n}})\big|_{x=0} = \mathbf{j}_x(x=0),$$

$$-\frac{1}{4\pi}(g_{i,2}^{\uparrow\downarrow} + g_{r,2}^{\uparrow\downarrow}\mathbf{n}\times)(\boldsymbol{\mu}_2'\times\mathbf{n} - \hbar\dot{\mathbf{n}})\big|_{x=d} = \mathbf{j}_x(x=d). \tag{6}$$

The quantity $\boldsymbol{\mu}_l'$ is the spin accumulation just inside the lth lead along the interface with F, which is related to the nonequilibrium electron spin density $\boldsymbol{\rho}_l$ there by $\boldsymbol{\mu}_l' = 2\boldsymbol{\rho}_l/D_l$, where D_l is the density of states. The spin accumulation $\boldsymbol{\mu}_l'$ is directed along the spin quantization axis $\mathbf{n}_l'$ just inside N_l and has a magnitude equal to the splitting between the electrochemical potential of electrons parallel ($\uparrow$) and electrons antiparallel ($\downarrow$) to $\mathbf{n}_l'$: $|\boldsymbol{\mu}_l'| = \mu_{l\uparrow}' - \mu_{l\downarrow}'$. Because the lead is, by assumption, a perfect spin sink, $\boldsymbol{\mu}_l'$ is generated electrically in the lead, which defines $\mathbf{n}_l'$.

The nonlinear Eqs. (4) and (5) together with the boundary conditions, Eq. (6), completely determine the evolution of $\mathbf{n}(\mathbf{r},t)$. For small angle dynamics, however, it suffices to linearize the bulk equations and boundary conditions: $\mathbf{n} \approx -\mathbf{z} + \delta\mathbf{n}$. To this end, writing $\mathbf{n} = (\sin\theta\cos\phi, \sin\theta\sin\phi, \cos\theta)$ in spherical coordinates, let us parametrize the nonequilibrium spin dynamics $\delta\mathbf{n}$ by the quantity

$$\Phi \equiv \sqrt{n_c}\,e^{-i\phi} \approx \sqrt{s/2}(\delta n_x - i\delta n_y) \tag{7}$$

(where $n_c/s \equiv 1+\cos\theta$), which vanishes in equilibrium ($\theta = \pi$). Equation (4) may be written, up to cubic order in Φ, as a Gross–Pitaevskii equation with a finite lifetime stemming from the Gilbert damping:

$$(i-\alpha)\hbar\partial_t\Phi = (\hbar\Omega - \hbar\nabla^2/2m)\Phi + \frac{K}{2}|\Phi|^2\Phi, \tag{8}$$

where $m = \hbar^2/2A$ is the kinetic mass, and, in the interest of small angle dynamics, we've neglected higher order, nonlinear terms in $\Phi/\sqrt{s}$. Here, the magnetic gap $\hbar\Omega = H - K$ plays the role of potential energy, while the anisotropy gives rise to interactions. The rotational invariance of the magnet around the z axis, presumed in free energy $\mathcal{F}$ above, is expressed by the invariance of Eq. (8) under the global gauge transformation $\Phi \to \Phi e^{-i\phi_0}$, where ϕ_0 is a constant. The bulk solution to Eq. (8), is a superposition of spin waves: $\Phi = \sum_{\mathbf{p}} c_{\mathbf{p}}\exp[-i\omega_{\mathbf{p}}t + i\mathbf{p}\cdot\mathbf{r}/\hbar]$ with complex frequency $\hbar\omega_{\mathbf{p}} \approx (1-i\alpha)(H - K + \mathbf{p}^2/2m) + \mathcal{O}(\alpha^2)$. The z component of the spin current Eq. (5) becomes, neglecting terms $\sim A\partial_x\Phi^4/s$:

$$j_i^{(z)} \equiv \mathbf{z}\cdot\mathbf{j}_i = \hbar\frac{\hbar}{m}\langle\Im[\Phi^*\nabla\Phi]\rangle = -\frac{\hbar^2}{m}|\Phi|^2\nabla\phi = \hbar n_c\mathbf{v}_s, \tag{9}$$

where $\mathbf{v}_s = -\hbar\nabla\phi/m$, in analogy with a superfluid current. The transport of z-spin therefore corresponds to a twist in the azimuthal coordinate ϕ of the spin density and is dc in the steady state.

Let us now consider how at zero temperature the spin density in F is excited by the spin accumulations in the metal leads. The boundary conditions Eq. (6) can be compactly expressed directly in terms of Φ :

$$-A\partial_x\Phi + \frac{g_{r,1}^{\uparrow\downarrow}}{4\pi s}(i\mu_1'\Phi + \hbar\partial_t\Phi) = 0, \quad x = 0,$$

$$A\partial_x\Phi + \frac{g_{r,2}^{\uparrow\downarrow}}{4\pi s}(i\mu_2'\Phi + \hbar\partial_t\Phi) = 0, \; x = d, \qquad (10)$$

where the spin accumulation is taken to be oriented in the z direction ($\boldsymbol{\mu}_l' = \mu_l'\mathbf{z}$), thereby respecting the rotational symmetry of F, and we've neglected the imaginary parts of the spin mixing conductances, which are in practice much smaller than the real. Via Eqs. (10), the normal metals bounding F determine the band structure of spin wave excitations as well as their lifetime, which is given by the transverse relaxation time $\tau_{\mathbf{p}} = -1/\Im[\omega_{\mathbf{p}}]$ for the mode with momentum $\mathbf{p} = \hbar(k\mathbf{x} + \mathbf{q})$ (where $k\mathbf{x}$ and $\mathbf{q} = q_y\mathbf{y} + q_z\mathbf{z}$ are the transverse and in-plane spin wave vectors, respectively). Were both normal metals perfectly poor spin sinks (so that angular momentum transfer across each interface is blocked by the normal metal spin accumulation in the steady state), the transverse wavevector $k \to k_m = m\pi/d$ ($m = 0, 1, 2\ldots$) would be quantized and real so that each mode decays over a timescale $\sim \hbar/\alpha(\hbar\Omega + A\mathbf{q}^2 + Ak_m^2)$. In this case, it is not possible to inject angular momentum from the metallic leads, and steady-state spin transfer across F is prohibited.

In our case, however, both normal metals are perfect spin sinks. Let us consider, for simplicity, a mirror-symmetric structure ($g_1^{\uparrow\downarrow} = g_2^{\uparrow\downarrow} = g^{\uparrow\downarrow}$), with spin accumulations applied along the z-axis: $\boldsymbol{\mu}_1' = \mu_1'\mathbf{z}$ and $\boldsymbol{\mu}_2' = \mu_2'\mathbf{z}$. Focusing a thin film ($d \ll l$, where $l = \sqrt{A/\hbar\Omega}$ is the effective exchange length) the lowest energy mode excited by the spin-transfer torque ($\mathbf{q} = 0$) is approximately monodomain. Integrating Eq. (8) over the thickness of the film, employing the boundary conditions, Eq. (10), and setting the imaginary part of ω to zero, one obtains $n_c/s = (\eta\mu_{\text{tot}}' - \hbar\Omega)/K$, with $\mu_{\text{tot}}' = \mu_1' + \mu_2'$. Here $\eta = \alpha'/(\alpha + 2\alpha')$, with $\alpha' = g_r^{\uparrow\downarrow}/4\pi sd$ as the spin-pumping contribution to the damping from each lead, is a measure of the efficiently of angular momentum injection by spin-transfer torque compared to dissipation into the lattice and leads. Because $n_c \geq 0$, μ_{tot}' must be equal to or larger than the gap $\hbar\Omega/\eta$ in order to induce magnetic dynamics in the steady-state. Physically, nonequilibrium physics in the leads creates a population inversion of electrons, which can only relax by the coherent emission of spin waves (i.e. the incitement of coherent magnetic dynamics) upon reaching a minimal threshold of μ_{tot}', in analogy to the pumping threshold for a laser; for this reason Berger [29] coined this type of process "swasing" (the spin wave analogue of lasing).

Below the swasing threshold ($\mu_{\text{tot}}' < \hbar\Omega/\eta$), the spin current through the structure vanishes. Above, the magnet is a spin-torque oscillator, precessing at a frequency $\Re[\hbar\omega] = \hbar\omega_r = \eta\mu_{\text{tot}}'$ and admitting a spin current across F. By symmetry, the spin currents flowing in the y and z directions vanish. The transverse components $j_x^{(x)}$, $j_x^{(y)}$ are ac; employing Eqs. (9) and (10), one has the remaining dc spin currents at the interfaces:

$$j_x^{(z)}(x = 0) = \frac{g^{\uparrow\downarrow}}{2\pi}(\mu_1' - \hbar\omega_r),$$

$$j_x^{(z)}(x = d) = -\frac{g^{\uparrow\downarrow}}{2\pi}(\mu_2' - \hbar\omega_r). \qquad (11)$$

When $\alpha = 0$, $j_x^z(x = 0) = j_x^z(x = d) \propto (\mu_1' - \mu_2')$, and all of the angular momentum is transferred from one side of the structure to the other without any losses into the F lattice.

4. Finite temperature dynamics

Equation (5) shows that at zero temperature, only spin perpendicular to $\mathbf{n}$ is transported inside F, which is a consequence of the fact that $\mathbf{n}$ is a unit vector that cannot accommodate any more or less angular momentum in the direction $\mathbf{n}$. Meanwhile, at finite temperatures, the spin density $\mathbf{s}$, as well as electrons in the leads and the lattice of F, fluctuates. The components of fluctuations of the $\mathbf{s}$ (corresponding to thermally activated spin waves) that are perpendicular to $\mathbf{n}$ average to zero, while the components parallel to $\mathbf{n}$ do not, resulting in a reduction of the average spin density $\langle\mathbf{s}\rangle = \tilde{s}\mathbf{n}$, where $\tilde{s} \leq s$ is a function of the temperature. This demagnetization provides a new channel for spin transport parallel to $\mathbf{n}$ which is markedly different from the zero-temperature dynamics of $\mathbf{n}$ described in the previous section. When out-of-equilibrium conditions (e.g. a temperature gradient) create spatial variations in $\tilde{s}$, exchange interactions between the moments of F act to restore equilibrium, resulting in the flow of angular momentum. In this section, we describe how thermal fluctuations transport angular momentum in the $N_l|F|N_2$ heterostructures under a minimal bias (i.e. in the linear response).

Thermally driven fluctuations of the spin density differ qualitatively from the microwave dynamics of $\mathbf{n}$ in a number of respects. First, whereas $\mathbf{n}$ is phase coherent (with a well defined precessional phase ϕ), phase information about thermally generated spin waves is lost over the ensemble average. For this reason, we refer to the former type of dynamics as coherent, and the latter as incoherent. Second, spin-transfer torque driven dynamics of $\mathbf{n}$ are generally long wavelength and precess at microwave frequencies $\sim (H - K)/\hbar$, thermally activated fluctuations

correspond a characteristic (de Broglie) wavelength $\Lambda = \sqrt{A/k_B T}$ and precess at frequencies $\sim k_B T/\hbar$, which, in room temperature ferromagnets, are usually much faster than microwave precession. Consequently, the dynamics of the fluctuations may differ considerably from that of **n**; for example, whereas the long wavelength dynamics of **n** are captured by the LLG phenomenology, dissipative dynamics of thermal fluctuations may no longer be described by Gilbert damping [30]. We shall, however, extrapolate the LLG phenomenology to thermal energies, with the understanding that results thereby obtained, while capturing key qualitative behavior, may fail to produce accurate quantitative predications.

To that end, two approaches to incorporating incoherent dynamics present themselves. The first is to introduce Langevin sources into the classical LLG phenomenology [22]. Agitations of the spin density, generated by thermal vibrations of the lattice, may be modeled by complementing H in Eq. (4) by a bulk stochastic field, while agitations created by Johnson–Nyquist noise at the N_l|F interfaces are captured by including separate stochastic fields in the boundary conditions, Eq. (6). This classical, stochastic account of incoherent dynamics provides an elegant description of spin transport meditated by subthermal spin wave excitations ($\hbar\omega < k_B T$), but must be cutoff at higher frequencies due to ultraviolet diverges in the theory. At temperatures larger than the spin wave gap, however, excitations above this bandwidth play an essential role.

The second approach is to recast magnetic dynamics within a quantum kinetic framework. In principle, the classical, stochastic framework may be expanded to include nonlinearities that give rise to magnon–magnon interactions, as well as elastic and inelastic scattering of thermal spin waves; such effects, however, can naturally grafted onto the framework of a semiclassical theory of bosons, which additionally does not suffer from the ultraviolet catastrophe present in the stochastic account. We therefore presently focus on outlining a quantum kinetic theory.

As a starting point, we quantize the spin density $\mathbf{s}/\hbar \to \hat{\mathbf{s}}$ according to the Holstein–Primakoff prescription [31]:

$$\hat{s}_z = \hat{\Phi}^\dagger\hat{\Phi} - s,\ \hat{s}_- = \sqrt{2s - \hat{\Phi}^\dagger\hat{\Phi}}\,\hat{\Phi}, \tag{12}$$

where $\hat{s}_- = \hat{s}_x - i\hat{s}_y$, and the fields $\hat{\Phi}$ satisfy $[\hat{\Phi}(\mathbf{r},t), \hat{\Phi}^\dagger(\mathbf{r}',t)] = \delta(\mathbf{r}-\mathbf{r}')$. The nondissipative dynamics may be obtained from the Hamiltonian, which, again neglecting dipole interactions, is given by:

$$\hat{\mathcal{H}} = \int d^3r \left(\frac{A}{s}\hat{\mathbf{s}}\cdot\nabla^2\hat{\mathbf{s}} - \frac{K}{s}\hat{s}_z^2 - H\hat{s}_z \right). \tag{13}$$

To lowest order in $\hat{\Phi}^\dagger\hat{\Phi}/s$ (which assumes small angle dynamics), the resulting Heisenberg equation of motion for $\hat{\Phi}$ is:

$$i\hbar\partial_t\hat{\Phi} = (H - K - \hbar^2\nabla^2/2m)\hat{\Phi}\ . \tag{14}$$

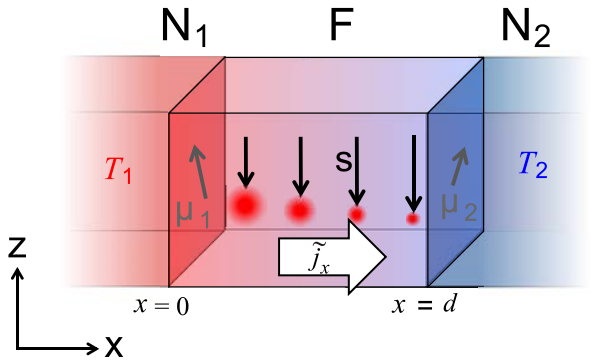

Fig. 2. At finite temperature, the N_1|F|N_2 can be thermally biased, complementing the spin accumulation. In the linear response regime, $\mathbf{n} = -\mathbf{z}$ in F, but thermally activated magnons support a spin current $\tilde{j}_x$ across F.

Next, we decompose $\hat{\Phi}$ into a scalar (Φ) and operator ($\hat{\varphi}$):

$$\hat{\Phi} = \Phi + \hat{\varphi}\ , \tag{15}$$

where we define $\langle\hat{\varphi}\rangle = 0$, so that $\langle\hat{s}_-\rangle \approx \langle\sqrt{2s}\hat{\Phi}\rangle = \sqrt{2s}\Phi$. Upon comparison with Eq. (7) in the limit $\alpha \to 0$, it is clear that $\hat{\Phi}$ here corresponds to coherent spin dynamics $\delta\mathbf{n}$, while the field $\hat{\varphi}$ fluctuates around $\mathbf{n} \approx -\mathbf{z}$. The scalar quantity Φ is a gauge field, resulting from tilting the order parameter **n** away from the z axis; excitations of this field are spin waves, with well-defined precessional phase and arbitrary amplitude. In contrast, the quanta of the field $\hat{\varphi}$ are magnons, each carrying $\hbar$ angular momentum in the $-\mathbf{n}$ direction. In our case, $\hat{\varphi}$-magnons are thermally activated fluctuations of **s** around the direction **n**, so that the averaging operation $\langle\ldots\rangle$ is performed over a thermal ensemble, again erasing phase information about each magnon. In the absence of coherent magnetic precession, $\mathbf{n} = -\hat{\mathbf{z}}$, Φ vanishes, and $\langle\hat{\mathbf{s}}\rangle = (s-n)(-\hat{\mathbf{z}}) = \tilde{s}\mathbf{n}$ (where $n \equiv \langle\hat{\varphi}^\dagger\hat{\varphi}\rangle$ is the thermal magnon density), thus demagnetizing the spin density to $\tilde{s} = s - n$. When **n** is slightly tilted away from equilibrium $s_z \approx -\tilde{s} + |\Phi|^2$, representing the combination of tilting and demagnetization, both of which act to reduce the spin density in the $-\hat{\mathbf{z}}$ direction. In the language of superfluidity, Φ plays the role of the superfluid wavefunction, while $\hat{\varphi}$ corresponds to the normal fluid component.

At the level of Eq. (14), the fields Φ and $\hat{\varphi}$ are uncoupled, which is a consequence of having neglected higher order terms in $\hat{\Phi}^\dagger\hat{\Phi}$ in the Holstein–Primakoff transformation that enter the Hamiltonian. These terms generate additional torques on the coherent magnetic dynamics that are absent at zero temperature. The incitement of coherent dynamics by a structural bias, even when assisted by these additional magnonic torques, occurs only beyond a threshold value. In contrast, for thermally activated magnons, which represent incoherent magnetic dynamics even in the absence of biasing, magnon spin and heat currents flow

across the $N_l|F$ interface in response to the smallest bias established in the N_l lead (though they may be absorbed by the lattice before they reach to other end). We will consider the steady state linear response of the heterostructure, wherein $\mathbf{n} = -\mathbf{z}$ and Φ vanishes.

4.1. Bulk transport

Let us now focus on the uncoupled bulk dynamics of the field $\hat{\varphi}$, the Heisenberg equation for which is obtained by averaging over and then subtracting the result from Eq. (14), yielding:

$$i\hbar\partial_t\hat{\varphi} = (H - K - \hbar^2\nabla^2/2m)\hat{\varphi}\,. \tag{16}$$

In order to include magnon–magnon interactions and disorder scattering, it is convenient to switch to a semiclassical kinetic description for magnons, which is achieved by first defining a magnon distribution function via a Wigner transformation:

$$f(\mathbf{r},\mathbf{p},t) \equiv \int d\mathbf{r}' e^{i\mathbf{p}\cdot\mathbf{r}'/\hbar}\langle\hat{\varphi}^\dagger(\mathbf{r}+\mathbf{r}'/2,t)\,\hat{\varphi}(\mathbf{r}-\mathbf{r}'/2,t)\rangle. \tag{17}$$

Gilbert damping and inelastic magnon scattering may enter phenomenologically at the level of a kinetic equation of motion for f (valid when the thermal de Broglie wavelength Λ is shorter than the mean free path for inelastic magnon scattering and $T/\partial_x T$):

$$\partial_t f + \frac{\mathbf{p}}{m}\cdot\nabla f = C[f] + \frac{f_P - f}{\tau_\alpha} + \frac{\overline{f} - f}{\tau_d}\,. \tag{18}$$

The terms on the lefthand side follow from Eq. (16), while the righthand side contains nonlinear and phenomenological contributions. The first term, $C[f]$ describes inelastic spin-preserving processes, including energy flow to and from the lattice and magnon–magnon collisions. The contribution from the latter, arising from both the anisotropy and exchange interactions, may be obtained by retaining higher order terms in $\hat{\varphi}^\dagger\hat{\varphi}/s$ in the Hamiltonian. The second term $\propto \tau_\alpha^{-1} = 2\alpha\epsilon_{\mathbf{p}}/\hbar$ (with $\epsilon_{\mathbf{p}} = \hbar\Omega + \mathbf{p}^2/2m$) on the righthand side phenomenologically describes dissipation by Gilbert damping (term $\propto -f$) and the accompanying thermal fluctuations of the lattice (term $\propto f_P$), which are connected by the fluctuation-dissipation theorem; these terms play the role of the bulk stochastic field in the classical theory. Here $f_P \equiv 1/[e^{\beta_P\epsilon_{\mathbf{p}}} - 1]$ is the effective phonon distribution function, with $\beta_P(x) = 1/k_B T_P(x)$ as the local inverse phonon temperature The last term $\sim \tau_d^{-1}(\epsilon_{\mathbf{p}})$ describes elastic disorder scattering, with $\overline{f}$ as the angular average of f in $\mathbf{p}$-space.

The local magnon-mediated spin current $\tilde{\mathbf{j}}_i = -\mathbf{n}\tilde{j}_i$ flowing across the structure is obtained from the kinetic equation, Eq. (18), by writing $f = \overline{f} + g$:

$$\tilde{j}_i = \hbar\int \frac{d\mathbf{p}}{(2\pi\hbar)^3}\frac{p_i}{m}g = \hbar\frac{2}{3}\int d\epsilon\frac{\sqrt{m/2}}{\pi^2\hbar^3}\tau\epsilon^{3/2}\nabla_i\overline{f} \tag{19}$$

where $\tau^{-1} = \tau_\alpha^{-1} + \tau_d^{-1}$, and we've neglected higher order contributions in τ. At temperatures well above the magnon gap $H - K$, the exchange interaction contribution to magnon–number–preserving magnon–magnon scattering rate dominates over that of the anisotropy, and the associated thermalization time is $\sim (k_B T/\hbar)(T/T_c)^3$, with T_c as the Curie temperature, which may be expected to be much faster than that due to spin relaxation processes. Spin-preserving inelastic processes thus force the distribution towards a local hydrodynamic equilibrium, which is described by a Bose–Einstein profile with a local magnon chemical potential $\mu(\mathbf{r})$ and temperature $T(\mathbf{r})$:

$$\overline{f}(\mathbf{r},\mathbf{p},t) \to f_{BE}(\mathbf{r},\mathbf{p}) \equiv \frac{1}{\exp[\beta(\mathbf{r})(\epsilon_{\mathbf{p}} - \mu(\mathbf{r}))] - 1}. \tag{20}$$

According to Eq. (18), spin and energy relaxation into the lattice dictates that in equilibrium, $f = f_P$, i.e. $\mu = 0$ and $T = T_P$ is uniform. Integrating Eq. (18) over momentum space and exploiting translation invariance in the yz plane ($\tilde{j}_y = \tilde{j}_z = 0$ and all quantities depend only on the coordinate x), we obtain a spin continuity equation that may be expanded around this equilibrium:

$$\hbar\dot{n} + \partial_x\tilde{j}_x = -G_\mu\mu - G_T(T - T_P), \tag{21}$$

where

$$G_\mu = \int d\epsilon\mathfrak{g}\frac{\hbar}{\tau_\alpha}\partial_\mu f_{BE}\,, \quad G_T = \int d\epsilon\mathfrak{g}\frac{\hbar}{\tau_\alpha}\partial_T f_{BE}\,, \tag{22}$$

evaluated at equilibrium, with $\mathfrak{g} = m^{3/2}\sqrt{(\epsilon - \hbar\Omega)/2}/\pi^2\hbar^3$ as the density of states. The linear response current is obtained by expanding Eq. (19) in μ and T:

$$\tilde{j}_x = -\sigma\partial_x\mu - \sigma S_b\partial_x T\,, \tag{23}$$

where

$$\sigma = -\hbar\frac{2}{3}\int d\epsilon\mathfrak{g}\frac{\epsilon}{m}\tau\epsilon^{3/2}\partial_\mu f_{BE}\,,$$

$$S_b = -\frac{\hbar}{\sigma}\frac{2}{3}\int d\epsilon\,\mathfrak{g}\frac{\epsilon}{m}\tau\epsilon^{3/2}\partial_T f_{BE} \tag{24}$$

are the bulk magnon conductance and spin Seebeck coefficients (again evaluated at equilibrium).

In the spirit of fast energy relaxation (compared to spin relaxation) into the lattice by spin-preserving inelastic processes, we suppose that $T(x) = T_P(x)$ everywhere, in which case the insertion of Eq. (24) into Eq. (21) yields an equation

for μ, which depends on the profile T_P. Provided that the magnons provided the bottleneck for heat transport across F, the high phonon thermal conductance translates into a linear profile for $T_P(x) = (x-d)\partial_x T_P$ (with $\partial_x T_P$ constant), which we shall assume here. Then, the bulk solution for μ becomes a linear combination of $e^{\pm x/\lambda}$, where $\lambda = \sqrt{\sigma/G_\mu}$ is the thermal magnon decay length. Supposing an energy independent mean-free path l_d, so that $\tau_d = \tau_d(\epsilon) = l_d/\sqrt{2\epsilon/m}$, Gilbert damping dominates when $\alpha \gg k_B\sqrt{TT_c}/\hbar s^{1/3} l_d$, in which case $\lambda \sim (T_c/T)^{1/2}/\alpha s^{1/3}$. When, on the other hand, disorder scattering dominates, $\lambda \sim (T/T_c)^{1/4}/\sqrt{l_d/s^{1/3}\alpha}$. In order to determine the full solution and therefore the spin current passing through the structure, we implement boundary conditions on the spin current at the normal metal/ferromagnet interfaces, which is the subject of the following section.

4.2. Interfacial transport

In general, under a bias a spin current flows across each interface with components both perpendicular to and parallel with $\mathbf{n}$ at that interface. The perpendicular spin currents at each interface is given by Eq. (6) (with finite temperature corrections to the real and imaginary parts of the spin mixing conductance, which are of the order n/s) [25]. In the presence of steady state coherent dynamics, this spin current is absorbed by $\mathbf{n}$ along the interface as a spin torque on $\mathbf{n}$, which is carried into the bulk of F by the current $\mathbf{j}_x$ in Eq. (5). In linear response, however, coherent dynamics are absent, and the perpendicular spin current entering F is absorbed by the lattice.

In contrast, at finite temperatures the interfacial spin current collinear with $\mathbf{n}$ is absorbed and carried into F by thermal magnons. The corresponding magnonic boundary conditions for collinear interfacial spin transport are given in terms of the magnon chemical potential and temperature, which are now well-defined in the local hydrodynamic approximation discussed above. To linear response in the spin accumulation $\boldsymbol{\mu}'_1$, magnon chemical potential, and left lead temperature T_1, this is (at $x = 0$):

$$\tilde{j}_x(x=0) = -g_1\delta\mu_1 - g_1 S_1 \delta T_1 \qquad (25)$$

where $\delta\mu_1 = \mu(x=0) + \boldsymbol{\mu}'_1 \cdot \mathbf{n}(x=0)$ and $\delta T_1 = T(x=0) - T_1$. The interfacial magnon spin conductance per area g_i and Seebeck coefficient S_1 are parametrized by the real part of the spin mixing conductance and may be expressed as derivatives of the quantity

$$M_1 = \frac{g_{r,1}^{\uparrow\downarrow}}{\pi}\int d\epsilon g\epsilon (f_1 - f)\big|_{x=0}, \qquad (26)$$

with $g_1 = \partial_\mu M_1$ and $g_1 S_1 = \partial_T M_1$ [25], all evaluated at equilibrium. Here $f_1 = 1/(e^{\beta_1 \epsilon_{\mathbf{p}}} - 1)$ is the effective equilibrium distribution of electron-hole pairs in N_l. The difference $(f_1 - f)$ in Eq. (27) reflects the competition between dissipation (term $\propto f$) of angular momentum into N_1 by magnon diffusion and fluctuations (term $\propto f_1$) of electrons just inside N_1. A similar boundary condition at $x = d$ holds.

Together with the bulk solutions, the boundary conditions completely determine the forms for $\mu(x)$ under a structural bias. The magnonic spin current flowing through, say, the left interface, may be expressed in terms of structural conductances (describing the linear response of the system to spin accumulations in the leads) and structural spin Seebeck coefficients (describing the linear response of the system to heating or cooling of the metal leads) [32,33], which is obtained by inserting into Eq. (26) the solution $\mu(x)$. Neglecting the Kapitza resistance so that the temperature is constant across the interfaces ($T_P(x=0) = T_1$ and $T_P(x=d) = T_2$), we obtain from Eq. (24)

$$\tilde{j}_x = g_{\rm tot}\left(\boldsymbol{\mu}'\cdot\mathbf{z} + \frac{\sigma S_b}{g}\partial_x T_P\right) 2\mathrm{Cosh}\left[\frac{x-d/2}{\lambda}\right] - \sigma S_b \partial_x T_P \qquad (27)$$

where $g_{\rm tot}^{-1} = g^{-1} + (\sigma/\lambda)^{-1}$ is the series conductance of the structure. For simplicity, we've taken the structure to be mirror symmetric ($g_1^{\uparrow\downarrow} = g_2^{\uparrow\downarrow} = g^{\uparrow\downarrow}$) with an antisymmetric bias $\boldsymbol{\mu}'_1 = -\boldsymbol{\mu}'_2 = \boldsymbol{\mu}'$ and $T_P = (x-d/2)\partial_x T_P$. Because there is no interfacial temperature drop, the current in Eq. (27) does not depend on the interfacial Seebeck coefficient S_1. However, the current at the $x = 0$ interface, $\tilde{j}_x(x=0) = g_{\rm tot}(\boldsymbol{\mu}'\cdot\mathbf{z} - S_b\lambda\partial_x T_P)$, suggests an *effective* temperature drop $\lambda\partial_x T_P$ away from the interface.

If, however, we relax the assumption of strong energy relaxation, the local magnon temperature T can deviate from the phonon temperature T_P, requiring that one additionally keep track of energy transport. The spin and heat currents passing through the structure then involve an interplay of interfacial and bulk Seebeck and Peltier effects, and the magnon chemical potential and temperature must be solved self-consistently.

We conclude this section by remarking that the quantum kinetic theory outlined above is analogous to the description of thermoelectric transport by itinerant electrons traversing a conducting N|F|N structure. Aside from the various length and timescales involved, magnon transport through the structure differs crucially from its electronic analog in three respects. First, magnons correspond to single channel, pure spin transport, whereas electron transport is two channel, requiring a separate treatment of spin majority ($\uparrow$) and minority ($\downarrow$) bands with respective local spin-dependent chemical potentials $\mu_\uparrow$ and $\mu_\downarrow$ and temperatures $T_\uparrow$ and $T_\downarrow$ [34]. (In practice, however, strong interspin and electron-phonon scattering forces the temperatures of the bands together [8]). Second, unlike the electron density, the local magnon density is not conserved

owing to Gilbert damping, though spin-orbit effects also break local conservation of the itinerant electron spin density. Last, in conducting structures, interfacial collinear spin transport is governed by the spin-dependent electron conductance, as opposed to the spin-mixing conductance that parametrizes collinear magnon transport here [25].

5. Conclusion

Thermally and electrically driven spin transport in magnetic insulators involve a number of lengthscales and interfacial and bulk effects (e.g. bulk and interfacial spin Seebeck effects). For low energy magnetic dynamics subject to Gilbert damping alone, these can be obtained from the bulk and interfacial damping, which may be measured by FMR measurements. The effects of Gilbert damping, elastic disorder scattering and inelastic spin-preserving processes on thermal magnons must be quantified by measurements of the total magnon temperature and density decay lengths, which is the focus of current research efforts [21,35].

At finite temperatures, we have focused on transport in the linear response regime, wherein coherent dynamics is absent. Beyond linear response, coherent dynamics may be excited by inducing an instability, as at zero temperature. As mentioned above, the presence of thermal magnons introduces spin torques on **n** in the bulk. These originate from two types of processes. The first is magnon–magnon scattering, which is rooted in the anisotropy; once the magnon chemical potential surpasses a threshold value, out-of-equilibrium magnons relax by exerting a local antidamping torque on **n**, which may be interpreted as a kind of internal swasing. The induction of coherent magnetic dynamics, the phase ϕ of which spontaneously breaks the U(1) rotational symmetry assumed around the z axis, by scattering from the incoherent thermal cloud of magnons may be interpreted as a type of Bose–Einstein condensation [36,37]. The second is a Berry phase effect, which originates from the exchange interaction. Here, as a magnon traverses a spatially varying spin texture $\mathbf{n}(\mathbf{r})$, it reorients so that it carries spin $-\hbar\mathbf{n}$; by conservation of angular momentum, the change in spin direction is imparted to **n**, resulting in a torque. By either mechanism, thermal magnons may assist in the incitement of coherent magnetic dynamics in F by swasing at an interface or may induce coherent dynamics by a structural thermal bias. An analysis of the full behavior beyond linear response at finite temperatures remains an active area of exploration.

This work was supported by the US DOE-BES under Award No. DE-SC0012190.

1. M. Johnson and R.H. Silsbee, *Phys. Rev. B* **55**, 1790 (1985).
2. Y. Ji, A. Hoffmann, J.S. Jiang, J.E. Pearson, and S.D. Bader, *J. Phys. D* **40**, 1280 (2007).
3. J.C. Slonczewski, *J. Magn. Magn. Mater*. **159**, L1 (1996).
4. J. Hirsch, *Phys. Rev. Lett*. **83**, 1834 (1999).
5. K. Ando, S. Takahashi, K. Harii, K. Sasage, J. Ieda, S. Maekawa, and E. Saitoh, *Phys. Rev. Lett*. **101**, 036601 (2008).
6. I.M. Miron, K. Garello, G. Gaudin, P.J. Zermatten, M.V. Costache, S. Auffret, S. Bandiera, B. Rodmacq, A. Schuhl, and P. Gambardella, *Nature* **476**, 189 (2011); doi: 10.1038/nature10309.
7. K. Uchida, S. Takahashi, K. Harii, J. Ieda, W. Koshibae, K. Ando, S. Maekawa, and E. Saitoh, *Nature* **455**, 778 (2008).
8. M. Hatami, G. Bauer, Q. Zhang, and P. Kelly, *Phys. Rev. Lett*. **99**, 066603 (2007).
9. H. Yu, S. Granville, D.P. Yu, and J.P. Ansermet, *Phys. Rev. Lett*. **104**, 146601 (2010).
10. X. Jia, K. Xia, and G.E.W. Bauer, *Phys. Rev. Lett*. **107**, 176603 (2011).
11. S. Hu, H. Itoh, and T. Kimura, *NPG Asia Mater*. **6**, e127 (2014).
12. A. Slachter, F.L. Bakker, J.-P. Adam, and B.J. Van Wees, *Nature Phys*. **6**, 879 (2010).
13. K. Uchida, J. Xiao, H. Adachi, J. Ohe, S. Takahashi, J. Ieda, T. Ota, Y. Kajiwara, H. Umezawa, H. Kawai G.E.W. Bauer, S. Maekawa, and E. Saitoh, *Nature Mater*. **9**, 894 (2010).
14. G.E.W. Bauer, E. Saitoh, and B.J. Van Wees, *Nature Mater*. **11**, 391 (2012).
15. A.V. Chumak, V.I. Vasyuchka, A.A. Serga, and B. Hillebrands, *Nature Phys*. **11**, 453 (2015).
16. C.W. Sandweg, Y. Kajiwara, A.V. Chumak, A.A. Serga, V.I. Vasyuchka, M.B. Jungfleisch, E. Saitoh, and B. Hillebrands, *Phys. Rev. Lett*. **106**, 216601 (2011).
17. A. Kapelrud and A. Brataas, *Phys. Rev. Lett*. **111**, 097602 (2013).
18. X. Jia, K. Liu, K. Xia, and G.E.W. Bauer, *Europhys. Lett*. **96**, 17005 (2011).
19. Y. Tserkovnyak and A. Brataas, *Phys. Rev. Lett*. **88**, 117601 (2002).
20. Y. Kajiwara, K. Harii, S. Takahashi, J. Ohe, K. Uchida, M. Mizuguchi, H. Umezawa, H. Kawai, K. Ando, K. Takanashi, S. Maekawa, and E. Saitoh, *Nature* **464**, 262 (2010); doi:10.1038/nature08876.
21. L.J. Cornelissen, J. Liu, R.A. Duine, J. Ben Youssef, and B.J. Van Wees, *arXiv.org, cond-mat.mes-hall* (2015).
22. S. Hoffman, K. Sato, and Y. Tserkovnyak, *Phys. Rev. B* **88**, 064408 (2013).
23. J. Xiao, G.E.W. Bauer, K.-c. Uchida, E. Saitoh, and S. Maekawa, *Phys. Rev. B* **81**, 214418 (2010).
24. H. Adachi, J. Ohe, S. Takahashi, and S. Maekawa, *Phys. Rev. B* **83**, 094410 (2011).
25. S.A. Bender and Y. Tserkovnyak, *Phys. Rev.B* **91** 140402 (2015).
26. T.L. Gilbert, *IEEE Trans. Magn*. **40**, 3443 (2004).
27. In practice, electrical and thermal biasing of the structure are mixed by, for example, Joule heating in the leads.
28. Y. Nazarov and G. Bauer, *Phys. Rev. Lett*. **84**, 2481 (2000).
29. L. Berger, *Phys. Rev. B* **54**, 9353 (1996).

30. E. G. Tveten, A. Brataas, and Y. Tserkovnyak, *ArXiv:1504.00511* (2015).
31. T. Holstein and H. Primakoff, *Phys. Rev*. **58**, 1098 (1940).
32. K. Uchida, M. Ishida, T. Kikkawa, A. Kirihara, T. Murakami, and E. Saitoh, *J. Phys. Condens. Matter* **26** 343202 (2014).
33. S.M. Rezende, R.L. Rodríguez-Suárez, R.O. Cunha, A.R. Rodrigues, F.L.A. Machado, G.A. Fonseca Guerra, J.C. Lopez Ortiz, and A. Azevedo, *Phys. Rev. B* **89**, 014416 (2014).
34. F.K. Dejene, J. Flipse, G.E.W. Bauer, and B.J. Van Wees, *Nature Phys*. **9**, 636 (2013).
35. B.L. Giles, Z. Yang, J. Jamison, and R. Myers, *ArXiv:1504.02808* (2015).
36. S.A. Bender, R.A. Duine, and Y. Tserkovnyak, *Phys. Rev. Lett*. **108**, 246601 (2012).
37. S.A. Bender, R.A. Duine, A. Brataas, and Y. Tserkovnyak, *Phys. Rev. B* **90**, 094409 (2014).